Title	Fabrication of elliptical mirror at nanometer-level accuracy for hard x-ray focusing by numerically controlled plasma chemical vaporization machining
Author(s)	Yamamura, Kazuya; Yamauchi, Kazuto; Mimura, Hidekazu et al.
Citation	Review of Scientific Instruments. 2003, 74(10), p. 4549-4553
Version Type	VoR
URL	https://hdl.handle.net/11094/85464
rights	This article may be downloaded for personal use only. Any other use requires prior permission of the author and AIP Publishing. This article appeared in Review of Scientific Instruments and may be found at https://doi.org/10.1063/1.1606531.
Note	

Fabrication of elliptical mirror at nanometer-level accuracy for hard x-ray focusing by numerically controlled plasma chemical vaporization machining

Kazuya Yamamura, Kazuto Yamauchi, Hidekazu Mimura, Yasuhisa Sano, Akira Saito, Katsuyoshi Endo, Alexei Souvorov, Makina Yabashi, Kenji Tamasaku, Tetsuya Ishikawa, and Yuzo Mori

---

Articles you may be interested in

Diffraction-limited two-dimensional hard-x-ray focusing at the 100 nm level using a Kirkpatrick-Baez mirror arrangement
Rev. Sci. Instrum. **76**, 083114 (2005); 10.1063/1.2005427

Fabrication of elliptically figured mirror for focusing hard x rays to size less than 50 nm
Rev. Sci. Instrum. **76**, 063708 (2005); 10.1063/1.1922827

Figuring with subnanometer-level accuracy by numerically controlled elastic emission machining
Rev. Sci. Instrum. **73**, 4028 (2002); 10.1063/1.1510573

The design and performance of an x-ray micro-focusing system using differentially deposited elliptical mirrors at the National Synchrotron Light Source
Rev. Sci. Instrum. **73**, 3464 (2002); 10.1063/1.1505656

The study of fabrication of the x-ray mirror by numerically controlled plasma chemical vaporization machining: Development of the machine for the x-ray mirror fabrication
Rev. Sci. Instrum. **71**, 4620 (2000); 10.1063/1.1322580

Fabrication of elliptical mirror at nanometer-level accuracy for hard x-ray focusing by numerically controlled plasma chemical vaporization machining

Kazuya Yamamura[a]
Research Center for Ultra-Precision Science and Technology, Graduate School of Engineering, Osaka University, Yamada-oka 2-1, Suita, Osaka 565-0871, Japan

Kazuto Yamauchi, Hidekazu Mimura, Yasuhisa Sano, and Akira Saito
Department of Precision Science and Technology, Graduate School of Engineering, Osaka University, Yamada-oka 2-1, Suita, Osaka 565-0871, Japan

Katsuyoshi Endo
Research Center for Ultra-Precision Science and Technology, Graduate School of Engineering, Osaka University, Yamada-oka 2-1, Suita, Osaka 565-0871, Japan

Alexei Souvorov and Makina Yabashi
SPring-8/Japan Synchrotron Radiation Research Institute (JASRI), Kouto 1-1-1, Mikazuki, Hyogo 679-5148, Japan

Kenji Tamasaku and Tetsuya Ishikawa
SPring-8/RIKEN, Kouto 1-1-1, Mikazuki, Hyogo 679-5148, Japan

Yuzo Mori
Research Center for Ultra-Precision Science and Technology and Department of Precision Science and Technology, Graduate School of Engineering, Osaka University, Yamada-oka 2-1, Suita, Osaka 565-0871, Japan

We established an efficient ultraprecise figuring process in which numerically controlled plasma chemical vaporization machining (NC-PCVM) and numerically controlled elastic emission machining (NC-EEM) are utilized serially. Intensity images of the x rays reflected by total reflection mirrors greatly fluctuate with respect to the figure error of spatial wavelength ranging from submillimeter to 10 mm. In NC-PCVM, figure errors for spatial wavelength range longer than 10 mm are removed efficiently by using the rotary electrode, and the spatial wavelength close to 1 mm can be corrected by using the pipe electrode. The residual figure error for the spatial wavelength close to 0.1 mm is finally removed by EEM. In this article, we describe the ultraprecise figuring process utilizing the NC-PCVM. Two elliptical mirrors for a Kirkpatrick–Baez (KB) microfocusing unit were manufactured by NC-PCVM using the rotary electrode and the pipe electrode in combination, and a figure accuracy higher than 3 nm ($p-v$) was achieved for the spatial wavelength range longer than 1 mm. The focusing properties of the two mirrors were evaluated at BL29XUL of SPring-8, and line focusing widths of 0.12 and 0.2 μm (full width at half maximum) were achieved at 15 keV. © *2003 American Institute of Physics.* [DOI: 10.1063/1.1606531]

I. INTRODUCTION

In third-generation synchrotron radiation facilities such as SPring-8, ESRF and APS, bright and coherent x-ray beams with low emittances are available. In order to utilize an x-ray beam preserving such excellent properties, x-ray optical devices having unprecedented degrees of accuracy are required. We realized a grazing incidence mirror having such accuracy by an advanced fabrication process of using numerically controlled plasma chemical vaporization machining (NC-PCVM) and numerically controlled elastic emission machining (NC-EEM) in sequence. Surface shape errors on the mirror, which affect the intensity distribution

and the wave front shape of the reflected x-ray beam, were analyzed by Fresnel–Kirchhoff diffraction integration in order to elucidate the spatial wavelength (λ_s) to be taken into account during figure-correction machining. In the analysis, Gaussian-shaped bumps having 1 nm height and width $w(2\sigma)$ ranging from 0.06 to 56 mm were superposed on the flat x-ray mirror in the longitudinal direction, and intensity fluctuation ratios $\Delta I/I_s$ and wavefront errors $\Delta\phi_s$ in the reflected x-ray beam ($E=15$ keV, $\theta=1.4$ mrad) were calculated and are shown in Fig. 1 as functions of bump width.[1] The error shapes in the spatial wavelength range from submillimeter to 10 mm order greatly affect the intensity profiles of reflected beams. Therefore, an effective machining technique of correcting the figure error of a short spatial wavelength (0.1 mm$<\lambda_s<10$ mm) is required. The figure error for the spatial wavelength over 10 mm affects the wave front

[a]Author to whom correspondence should be addressed; electronic mail: yamamura@upst.eng.osaka-u.ac.jp
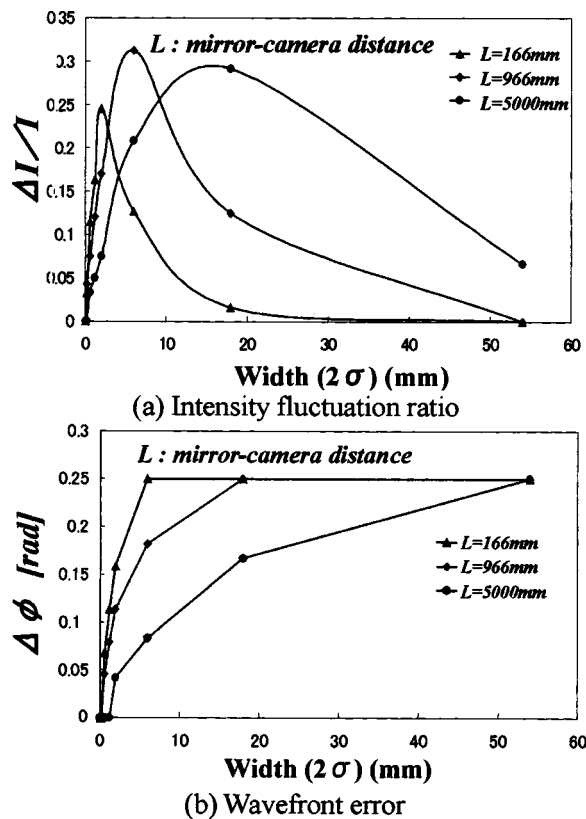
FIG. 1. The relationship between bump width and (a) intensity fluctuation and (b) wave front error of reflected beam.

error, and the value of the phase error is close to the value geometrically defined as $4\pi h \sin\theta/\lambda$ (*h*: bump height, θ: glancing angle) for longer spatial wavelength. The strategy proposed here for manufacturing ultraprecise mirrors is to correct figure errors in the spatial wavelength range from the clear aperture size to 1 mm by NC-PCVM, and those in the shorter spatial wavelength range by NC-EEM.

II. GENERAL VIEW OF NC-PCVM

PCVM is a chemical machining method utilizing atmospheric pressure plasma.[2–4] Reactive gas molecules supplied to the plasma region are decomposed into high-density neutral radicals having high chemical reactivity, by the
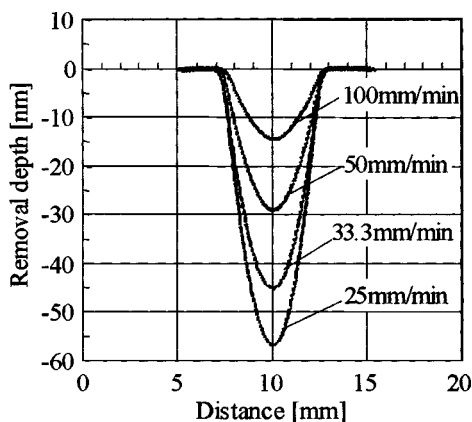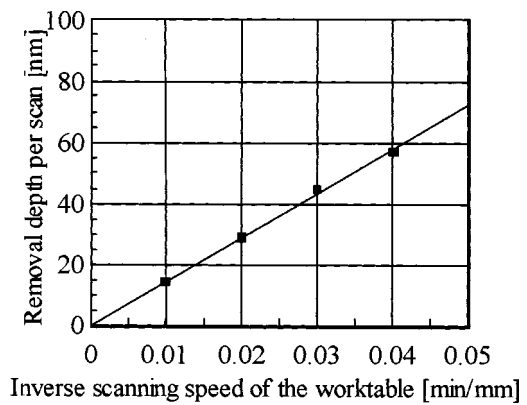

FIG. 3. Relationship between inverse scanning speed of the worktable and removal depth of silicon in one-pass scanning.

atmospheric-pressure rf plasma locally generated in the gap space between the electrode and the workpiece. Then, surface atoms are removed as volatile species by reaction with the neutral radicals generated in the plasma. As understood from the removal mechanism in PCVM, the required shape can be obtained without degrading the original functional properties of the material from the crystallographic viewpoint. Therefore, PCVM is an effective machining method not only for total-reflection mirrors but also for Bragg diffraction devices.

To manufacture ultraprecise mirrors, premachined shapes must be measured with an accuracy better than the required accuracy. When the shape of the mirror is not steeply curved, both a microscopic interferometer and a large-area Fizeau interferometer are used in combined stitching interferometry for the measurement.[1,5] The absolute surface shape of the reference plane of the Fizeau interferometer is calibrated by the three-flat test. Then, it is possible to obtain accurate shape data over spatial wavelengths ranging from the submillimeter to the 100 mm order by the combined stitching interferometry using the microscopic interferometer and the large area interferometer. Distribution of the dwelling time of the plasma necessary for selective correction of the figure error is calculated by deconvolution using the shape of the removal spot. Then, the numerically controlled figure correction can be carried out by controlling the scanning speed of the worktable calculated as inverse values of

FIG. 2. Profiles of processed groove at various scanning speed conditions.
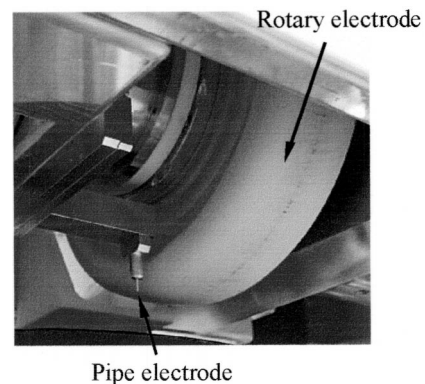

FIG. 4. Photograph of the rotary electrode and the pipe electrode equipped on the NC-PCVM machine.

FIG. 5. Profiles of the removal spot on the silicon surface.

TABLE I. Constant values of ellipse equation $x^2/a^2 + y^2/b^2 = 1$ and incident angles θ_i of designed mirrors.

f (mm)	a (m)	b (mm)	θ_i (mrad)
300	500.15	24.25	1.4
150	500.15	18.09	1.47

FIG. 7. The cross-sectional shape of elliptical mirrors installed in the KB focusing unit.

the dwelling times. Figure 2 shows depth profiles in groove machining of the silicon surface at various scanning speeds. Compositions of the process gas are CF_4 (0.01%), O_2 (0.01%), and helium balance. Groove depths are seen to increase with decreasing scanning speed without changing the groove width. Figure 3 shows the relationship between dwelling time of the plasma and removal depth in the case of one-pass scanning. The removal depth is so highly proportional to the dwelling time that a very slight removal depth of nanometer order can be precisely controlled in this method.

A small pipe electrode of 1 mm diameter is installed at the side of the rotary electrode, in case of correcting the figure error with high spatial resolution. In using the pipe electrode, reaction products in the PCVM process are removed through the pipe by a suction pump. Figure 4 shows the rotary electrode (ϕ 200 mm) and the pipe electrode actually equipped on the NC-PCVM machine. During rotating electrode processing, the pipe electrode is detached. Figure 5 shows typical removal spot shapes obtained on the silicon surface using the: (a) rotary electrode and (b) pipe electrode, having the diameters of about 20 and about 2 mm, respec-
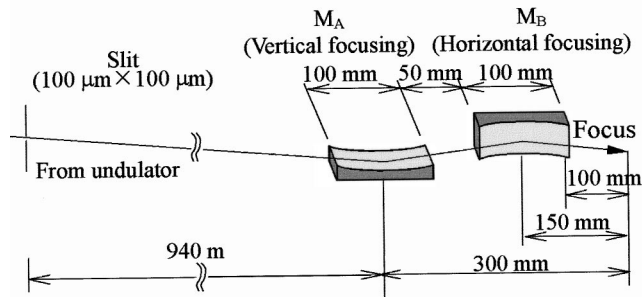

FIG. 6. Layout of the two-dimensional focusing system for hard x ray using a Kirkpatrick–Baez (KB) mirror arrangement.
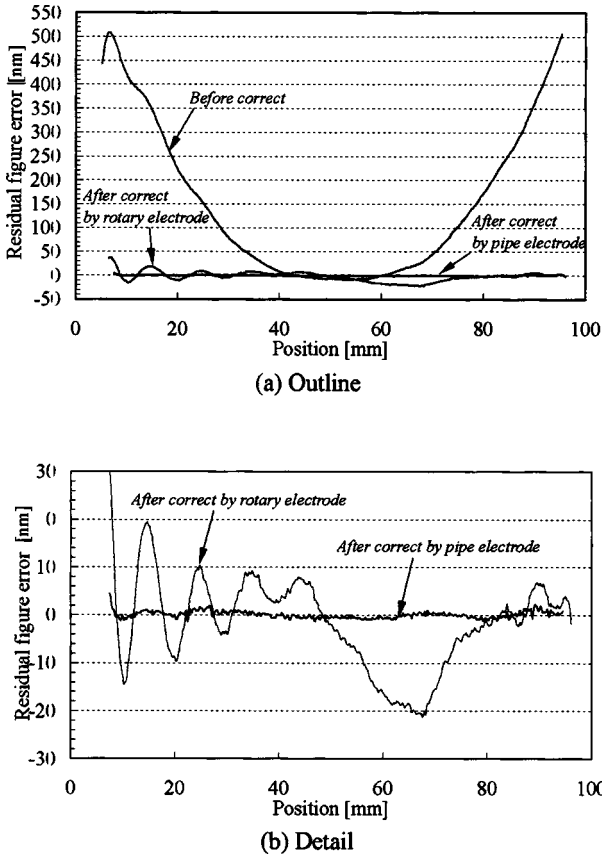

(a) Outline

(b) Detail

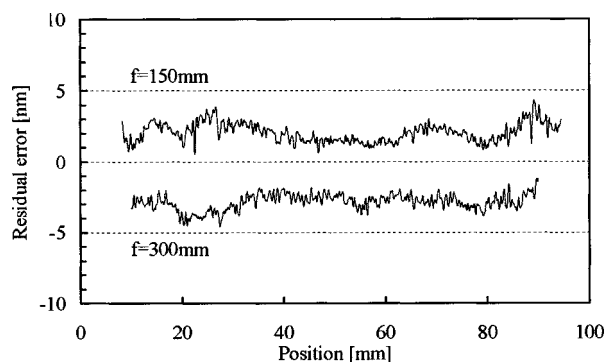FIG. 8. Residual figure errors of the elliptical mirror in each stage of NC-PCVM.

FIG. 9. Final residual figure errors of two elliptical mirrors fabricated by NC-PCVM.

tively. Removal rates were: (a) 2 mm^3/h and (b) 7 $\times 10^{-3}$ mm^3/h, respectively.

III. FIGURING OF ELLIPTICAL MIRROR

We evaluated the figuring performance of the NC-PCVM process by manufacturing elliptical mirrors for hard x-ray focusing. In a conventional hard x-ray focusing system, approximate ellipses are realized by elastic deformation of flat mirrors using benders. In contrast, we manufacture an exact elliptical shape on the mirror surface without bending. Figure 6 shows the layout of a two-dimensional focusing system for hard x-ray beams using a Kirkpatrick–Baez mirror arrangement applicable to BL29XUL of SPring-8.[6] In this unit, two elliptical mirrors for vertical and horizontal focusing are installed. Mirrors are made of single-crystalline silicon without any coating material and have the same size of 100 mm$\times$50 mm$\times$10 mm. Focal lengths of the two mirrors are 300 mm for vertical focusing and 150 mm for horizontal focusing, respectively. Ellipse parameters and average glancing angle of each mirror are shown in Table I. Figure 7 shows the cross-sectional shape of the two elliptical mirrors along the direction of the incident x-ray beam.

In the fabrication process of the mirror by NC-PCVM, rough figuring in the long spatial wavelength range is carried out using the rotary electrode. Then, shape error in the short spatial wavelength range is corrected using the pipe electrode. Figure 8 shows residual figure errors of the elliptical mirror for horizontal focusing in each stage of NC-PCVM. In the correction process using the rotary electrode, the figure
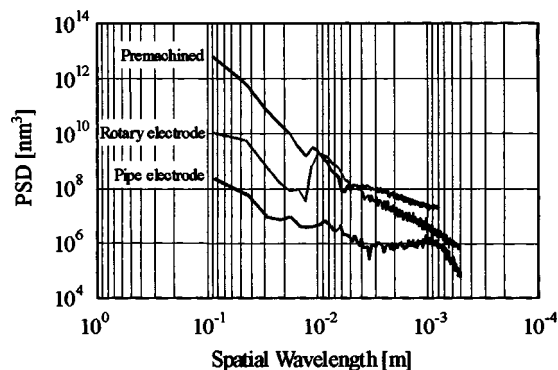

FIG. 10. Power spectral density plot of residual figure errors in the correction process by NC-PCVM.
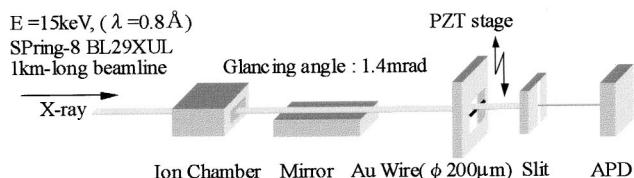

FIG. 11. Schematic drawing of the measurement of the focused beam profile by the wire scanning.

error of 50 nm or less is achieved in the spatial wavelength range longer than 10 mm. After the correction process using the pipe electrode, a figure accuracy as high as 3 nm ($p-v$) is achieved over the region as long as 90 mm in the longitudinal direction, as shown in Fig. 9.
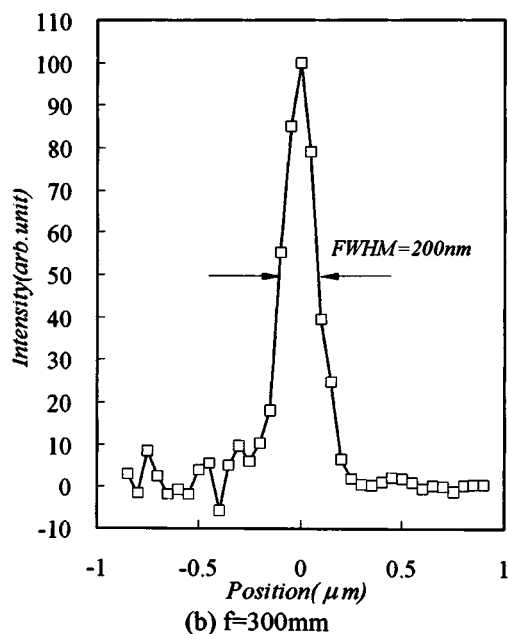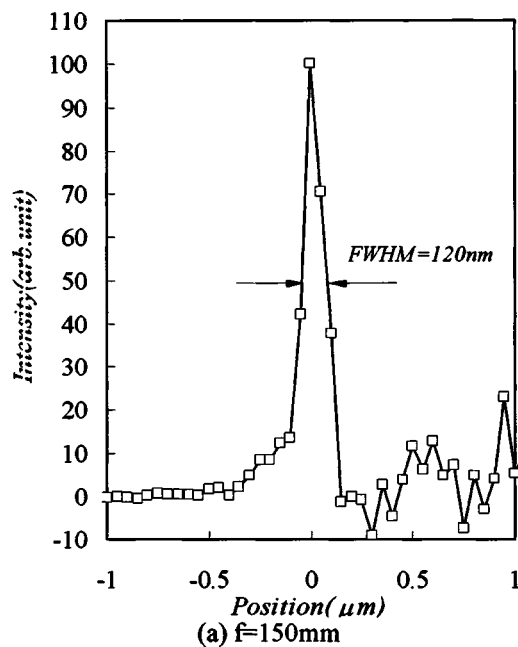

FIG. 12. Line focused beam profiles measured by Au wire (ϕ 200 μm) scanning ($E = 15$ keV, $\theta = 1.4$ mrad). Mirror material is single crystal silicon without metal coating of the surface.

In the conventional polishing process, there are many process parameters to be controlled, and they interact with each other in a complex manner so that it is very difficult to keep the removal rate stable for the total duration of machining; therefore it is difficult to achieve a high figure accuracy such as that of nanometer order. On the contrary, in the case of NC-PCVM processes, the controlled parameter is only the scanning speed of the worktable as long as gas concentration and rf power are kept constant. Consequently, the nanometer-order figure accuracy can be easily achieved with the advantage of a noncontact process in which there is little influence of machine deformation induced by external disturbances such as vibration and temperature fluctuation. Therefore, the NC-PCVM process has great advantage over the mechanical polishing process in the manufacture of optical devices which require ultimate accuracy, such as x-ray mirrors.

Figure 10 shows the power spectral density plot of residual figure error in the correction process by NC-PCVM. The lower limit of the spatial wavelength of figure-correctable error profiles is known to correspond to about half the size of the unit removal spot, which are about 10 and about 1 mm for the rotary electrode and the pipe electrode, respectively.

Figure 11 shows the experimental setup for measuring the focused beam profile at BL29XUL of SPring-8. The focused beam profile was measured by a wire scanning method in which a gold wire (ϕ 200 μm) was employed and scanned with 50 nm steps using the piezo stage. Beam intensity is detected by an avalanche photodiode and is normalized by the incident beam intensity detected using an ion chamber placed before the focusing mirror. Figure 12 shows line focused beam profiles of two elliptical mirrors. The line focused beam widths of the mirrors of 150 mm and of 300 mm focal length are 0.12 and 0.20 μm (full width at half maximum) at 15 keV, respectively.

In this study, we manufactured elliptical mirrors by NC-PCVM, and submicron focusing width was realized. Figure error components for the spatial wavelength of submillimeter order are planned to be corrected with NC-EEM. In the NC-EEM process, the figure accuracy of subnanometer order with surface roughness of atomic order can be realized. However, the removal rate in EEM is not so high. We systematized a high efficient manufacturing process of optical devices with perfectly corrected figure error for the spatial wavelength longer than submillimeter order by combining NC-EEM with NC-PCVM which has a high removal rate.

ACKNOWLEDGMENTS

[1] Y. Mori et al., Proc. SPIE **4501**, 30 (2001).
[2] Y. Mori, K. Yamamura, K. Yamauchi, T. Yoshii, K. Kataoka, K. Endo, K. Inagaki, and H. Kakiuchi, Nanotechnology **4**, 225 (1993).
[3] Y. Mori, K. Yamamura, and Y. Sano, Rev. Sci. Instrum. **71**, 4620 (2000).
[4] Y. Mori, K. Yamauchi, K. Yamamura, and Y. Sano, Rev. Sci. Instrum. **71**, 4627 (2000).
[5] K. Yamauchi et al., Rev. Sci. Instrum. **74**, 2894 (2003).
[6] P. Kirkpatrick and A. V. Baez, J. Opt. Soc. Am. **38**, 766 (1948).